INL/CON-15-34058
PREPRINT

Uncertainty Quantification of Calculated Temperatures for Advanced Gas Reactor Fuel Irradiation Experiments

16th International Topical Meeting on Nuclear Reactor Thermalhydraulics (NURETH-16)

Binh T. Pham, Grant L. Hawkes,
Jeffrey J. Einerson

August 2015

UNCERTAINTY QUANTIFICATION OF CALCULATED TEMPERATURES FOR ADVANCED GAS REACTOR FUEL IRRADIATION EXPERIMENTS

Binh T. Pham, Idaho National Laboratory

Grant L. Hawkes, Idaho National Laboratory

Jeffrey J. Einerson, Idaho National Laboratory

Manuscript Contact: Name: Binh T. Pham

Phone Number: 805-448-1383

Email: binh.pham@inl.gov

Total Number of Pages: 22

Total Number of Tables: 2

Total Number of Figures: 9

UNCERTAINTY QUANTIFICATION OF CALCULATED TEMPERATURES FOR ADVANCED GAS REACTOR FUEL IRRADIATION EXPERIMENTS

Binh T. Pham*, Grant L. Hawkes, and Jeffrey J. Einerson
Idaho National Laboratory
2525 Fremont Avenue, Idaho Falls, Idaho 83415
binh.pham@inl.gov; grant.hawkes@inl.gov; jeffrey.einerson@inl.gov

ABSTRACT

This paper presents the quantification of uncertainty of the calculated temperature data for the Advanced Gas Reactor (AGR) fuel irradiation experiments conducted in the Advanced Test Reactor at Idaho National Laboratory in support of the Advanced Reactor Technology Research and Development program. The predicted temperatures with associated uncertainty for AGR tests using the ABAQUS finite element heat transfer code are used for validation of the fission product transport and fuel performance simulation models. To quantify the uncertainty of calculated temperatures, this study identifies and analyzes model parameters of potential importance to the predicted fuel temperatures. The selection of input parameters for uncertainty quantification is based on the ranking of their influences on variation of temperature predictions. Thus, selected input parameters include those with high sensitivity and those with large uncertainty. Propagation of model parameter uncertainty and sensitivity is then used to quantify the overall uncertainty of calculated temperatures. The sensitivity analysis performed in this work went beyond the traditional local sensitivity. Using experimental design, analysis of pairwise interactions of model parameters was performed to establish sufficiency of the first-order (linear) expansion terms in constructing the response surface. To achieve completeness, uncertainty propagation made use of pairwise noise correlations of model parameters. The AGR-2 overall fuel temperature uncertainties reported here are less than 5% (or 60˚C).

KEYWORDS
Thermal analysis, uncertainty quantification, and sensitivity coefficient.

* Corresponding author

I. INTRODUCTION

Several Advanced Gas Reactor (AGR) irradiation experiments are being conducted in the advanced test reactor (ATR) within the Advanced Reactor Technology Fuel Development and Qualification Program. The main objective of the fuel testing campaign is to qualify tristructural isotropic (TRISO) coated particle fuel for use in high temperature gas reactors (HTGRs) [1]. These tests also provide the necessary irradiation data to support development and validation of fuel performance and fission product transport models and codes. The AGR test trains are comprised of multiple independently monitored capsules stacked on top of each other used to assess the fuel performance under various fabrication and irradiation conditions. Each capsule consists of fuel compacts placed in a graphite cylinder shrouded by a hafnium and stainless steel layer and capsule shell. The fuel being tested in AGR capsules are TRISO coated fuel particles containing uranium oxycarbide and uranium dioxide fuel produced in the United States at different production scales, which serve as the foundation for fabrication on a commercial scale. Each AGR experiment is irradiated for two to three years resulting in up to approximately 620 effective full power days (EFPDs) as for the first experiment, AGR-1.

For fuel temperature control, the AGR experiments are instrumented with thermocouples (TCs) terminating in a graphite sample holder and their readings are maintained at predefined levels by varying the neon and helium gas mixture flowing through the two gaps: one between the fuel stack and the graphite holder hole, and one between the graphite holder and the stainless steel shell (called the control gas gap). According to the test specification, TCs used in AGR capsules have an as-installed accuracy of ±2% of reading. To prevent unwanted test article interactions and possible unwanted failures, no object or material other than specifically designed compact matrix, graphite test articles and holders, and sweep gas should come into contact with the irradiation test fuel. Therefore, there are no direct temperature measurements for fuel compacts. The ABAQUS code's finite element-based thermal model is created to predict the daily average volume-average fuel temperature (VA FT) and peak fuel temperature (peak FT) in each of AGR capsules for the entire irradiation [2]. This thermal model involves complex physical mechanisms (i.e., graphite holder and fuel compact shrinkage or swelling) and properties (i.e., conductivity and density). Therefore, the temperature predictions are affected by uncertainty in input parameters and by incomplete knowledge of the underlying physics leading to modeling assumptions. Therefore, alongside with the deterministic predictions from a set of input thermal conditions, information about prediction uncertainty is instrumental for the ART program decision-making. Well defined and reduced uncertainty in model predictions helps increase the quality of and confidence in the AGR technical findings [3, 4].

This paper focuses on the uncertainty quantification of fuel temperatures predicted by the ABAQUS-based thermal models due to the input uncertainties. The acceptable fit between TC readings and model predictions over the entire irradiation supports the negligible model bias assumption [4]. To quantify fuel temperature uncertainty, ABAQUS thermal model input parameters of potential importance are identified. A set of parameters is selected including those with high sensitivity and/or those with large uncertainty. The parameter uncertainties and sensitivity coefficients are combined to quantify the overall uncertainty of temperature outputs. It is also important to emphasize that the input uncertainties are dynamic accounting for the effect of unplanned events and changes in thermal properties of capsule components over extended exposure to high temperature and fast neutron irradiation.

II. THERMAL MODEL FOR AGR CAPSULE

ABAQUS-based (Version 6.8-2), three-dimensional finite-element thermal models are created for each AGR capsule to predict daily averages of VA FT, peak FT, and TC temperatures for the entire irradiation period when the ATR core is at power. Fig. 1 depicts a sideways cutaway view of ~350,000 eight-node hexahedral brick finite element mesh for each capsule with the ATR primary cooling water as the ultimate heat sink. The governing equations of steady-state conduction and radiation heat transfer are used for the thermal models of AGR-1 and AGR-2 capsules [2, 5, 6]. The fission power largely generated in the fuel compact and graphite sample holder is conducted out to the ATR primary cooling water through the two gas gaps. The radiation heat transfers occur from the graphite holder to the stainless-steel retainer, graphite holder to thru-tubes, and thru-tubes to the stainless-steel retainer. Fig. 2 shows the typical fuel temperature distribution in cutaway view of three fuel stacks for each day and each of AGR-1 and AGR-2 capsules. Apparently, fuel temperature peaks near the center line and varies by more than 250°C ranging between 750°C and 1013°C.

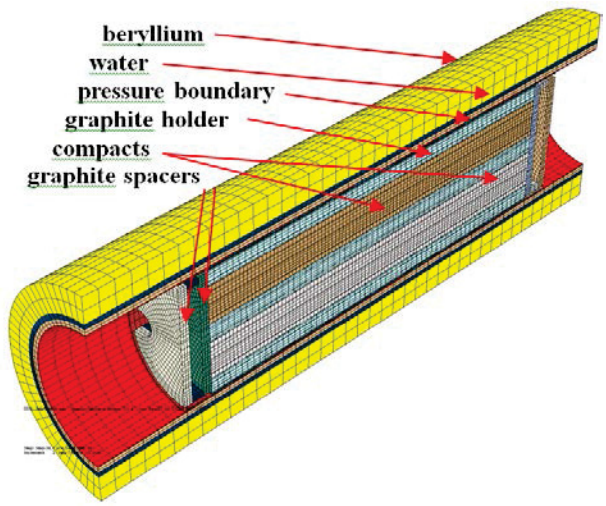

Fig. 1. Sideways cutaway view of mesh for an AGR capsule.

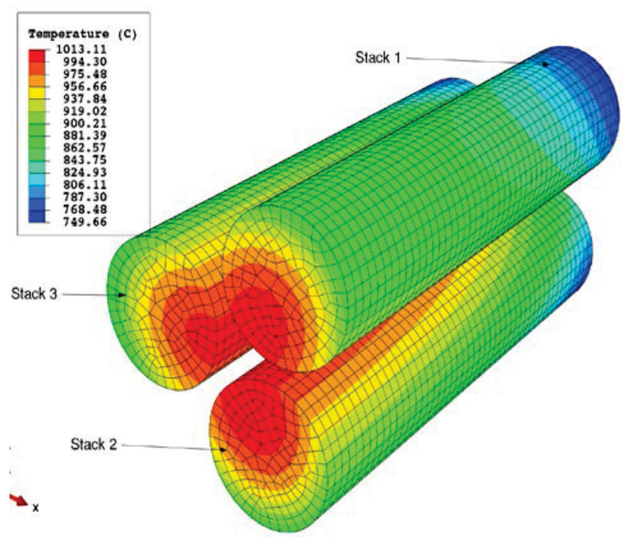

Fig. 2. Temperature distribution in cutaway view of three fuel stacks.

The main time-series inputs to the capsule thermal model are components' daily heat rates and neutron fast fluences calculated from the as-run depletion analysis [7] and daily gas compositions of the helium-neon mixture (neon fraction). The fast neutron fluence is needed for calculation of the thermal conductivity and for estimation of the control gap size variations during irradiation [2]. Even though the acceptable fit between TC readings and model predictions over the entire irradiation supports the negligible model bias assumption, the following model assumptions will likely contribute to predicted fuel temperature uncertainties:

1. The control gap is evenly and linearly changing over the entire irradiation as function of fast fluence.
2. Heat rates from components (excluding fuel compacts divided into two nodes) and fluences are spatially constant and vary only with time for each capsule.
3. Graphite and compact thermal conductivity vary with fluence and temperature, which are taken from legacy experiment correlations and scaled for AGR material density.
4. Gas mixture thermal conductivity is determined by kinetic theory of gases using pure gas properties of helium and neon to determine mixture properties.
5. Because the thermal capacitance of the sweep gas is very low, advection is not considered in the sweep gas, and it is modeled as stationary.
6. Emissivity estimates for radiation heat transfers.
7. There is no axial heat conduction from one capsule to the next.

III. UNCERTAINTY QUANTIFICATION FOR FUEL TEMPERATURE

III.A. Uncertainty Quantification Approach

In general, uncertainty in the prediction of a simulation model arises from two main sources: input uncertainty and model uncertainty. This is assuming that the numerical errors can be eliminated by the use of adequate spatial resolution in computing code. Subsequently, the overall uncertainty of simulation model predictions in terms of variance can be expressed as:

$$\sigma_T^2 = \sigma_p^2 + \sigma_B^2 \tag{1}$$

where: σ_T^2 is the overall uncertainty of predicted temperature in terms of variance, σ_p^2 is the input uncertainty in terms of variance, and σ_B^2 is the model bias in terms of variance. Model uncertainty usually arises from assumptions associated with the mathematical form or structure of the model. While no direct measurements of fuel temperature are available, the temperatures measured by TCs embedded in the graphite sample holder are used to calibrate the thermal model for each capsule. These TC measurements are rigorously scrutinized to identify any abnormal behavior indicating instrumental failures [8]. This helps prevent the use of bad TC readings for model calibration. The rationale for negligible model uncertainty of AGR calculated temperatures is based on consistency between measured and calculated temperatures at TC locations and on significant correlation between fuel temperature and temperature sensitive fission product release-to-birth ratios over the extended irradiation as discussed in [4]. As a result, this paper focuses on the uncertainty quantification of fuel temperatures in each AGR capsule predicted by the ABAQUS-based thermal models due to the input parameter uncertainties.

Input uncertainty refers to incomplete knowledge of correct values of model inputs, which exists independently with any model, but will impact the uncertainty of model prediction. To quantify the input uncertainty of AGR calculated temperatures, ABAQUS model input parameters of potential importance are identified. Identification has two parts: (1) using sensitivity analysis, determine parameters that the modeling is most sensitive to, and refine the estimates of these sensitivities, and (2) using expert judgment, determine parameters with the largest uncertainties and estimate these uncertainties. However, the spatial differential equations for steady-state conduction and radiation heat transfers used in AGR capsule thermal models make it impossible to derive a unique analytical formula to calculate output uncertainty from input variations over the whole AGR experimental condition domain. Additionally, the standard Monte Carlo technique is impractical because of the necessity of requiring hundreds of thousands of simulations to estimate the overall output temperature uncertainty with satisfactory accuracy. Therefore, assuming the predicted temperature can be expressed by the weighted summation of input parameters, the parameter uncertainties and sensitivity coefficients are combined and propagated to quantify the uncertainty of calculated temperatures as follows [9]:

$$\sigma_p^2 = \sum_{i}^{n} a_i^2\, \sigma_i^2 + \sum_{i}^{n} \sum_{j \# i}^{n} \rho_{ij} a_i\, \sigma_i a_j \sigma_j \qquad (2)$$

where: a_i^2 is the square of the sensitivity coefficient for parameter *i*, σ_i^2 is the uncertainty of input parameter *i* in terms of variance, and ρ_{ij} is the correlation coefficient for input parameters *i* and j. All terms necessary for fuel temperature uncertainty quantification using Eq. 2 are discussed in following subsections.

III.B. Sensitivity Analysis

The parameter sensitivity defines how the predicted temperature would be influenced by changes in an input parameter. The uncertainty of the model output increases as the sensitivity coefficient of an input parameter increases. The input sensitivity analysis was performed for an AGR capsule to assess the impact of input variation on calculated fuel temperatures [5, 6]. A series of cases was compared to a base case by varying different input parameters to the ABAQUS finite element thermal model. The bar charts in Fig. 3 represent the variations of peak FT (left plot) and VA FT (right plot) when each input parameter varies by ±10%. The variations are sorted from largest to smallest for peak FT. The most sensitive parameters are heat rate in the fuel compacts, control gas neon fraction, and control gap size indicating by the largest variation of calculated fuel temperatures. The next four are heat rate in the graphite, fuel thermal conductivity, graphite thermal conductivity, and gap conductivity between compact and graphite holder. These sensitivities combined with parameter uncertainties are used to determine the five most influential inputs for calculated temperature uncertainties: heat rate in the fuel, control gas neon fraction, control gap size, fuel thermal conductivity, and graphite thermal conductivity. The first three are because of their high sensitivity and the last two because of their high parameter uncertainty.

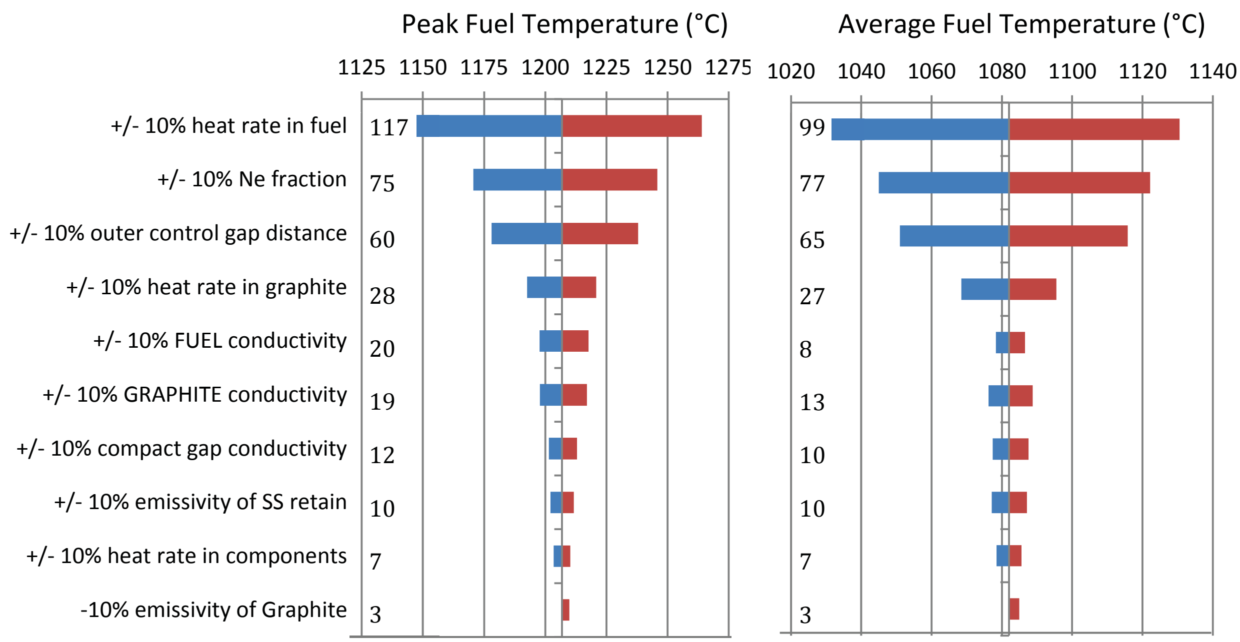

Fig. 3. Sensitivities for peak and volume-average fuel temperatures.

III.B.1. Input parameter interaction

The statistical experimental design was used to develop the set of simulation runs necessary to estimate main effects and pairwise interactions of the five important input variables. This requires 51 runs of the ABAQUS code for one thermal condition (i.e., one day) as follows: a baseline run for nominal inputs, 10 runs for separate input variation of ±10% to estimate main effects, and 40 runs for variation of all input pairs to assess their interactions. Then, the JMP® module of SAS® [10] is used to build a surrogate response surface model for each of the calculated temperatures in order to determine which input terms have significant impacts. The estimated parameter coefficients are treated as sensitivities that estimate the rate of change of temperature with regard to the input change. The full response surface model containing first order terms and second order terms (square and pairwise) is constructed and studied for each of calculated temperature as follows [11]:

$$T_f = a_0 + \sum_{i=1}^{5} a_i x_i + \sum_{i=1}^{5} \sum_{j=1}^{5} a_{ij}\, x_i x_j \quad (3)$$

where T_f is fuel temperature (volume-average or peak); a_i and a_{ij} are parameter estimates for first and second order terms respectively; x_i and x_j are five selected model inputs such as *HR* is fuel heat rate, *GG* is the control gap size, *NeF* is neon fraction, *GC* is graphite thermal conductivity, and *FC* is fuel compact thermal conductivity. This response surface function fits very well to calculated fuel temperatures. Fig. 4 shows parameter estimates (Eq. 3) sorted from the largest to the smallest for VA FT. Most of parameter estimates are significantly different from zero, as indicated by the small Prob>|t| values in the last column to the right. However, the pink bar chart showing the temperature variation due to input change indicates that only five main effects are dominant. The square of neon fraction is the most significant among the second order terms, but has insignificant influence on output temperature. This allows for exclusion of all second order terms in Eq. 3. Thus, the calculated fuel temperature can be expressed as a linearized approximation of input variables and, subsequently, the input uncertainties can be propagated using Eq. 2. This linear function is given as:

$$T_f = a_0 + a_1 HR + a_2 GG + a_3 Nef + a_4 GC + a_5 FC \quad (4)$$

Sorted Parameter Estimates

Term	Estimate	Std Error	t Ratio	Prob>|t|
FHR_s1	0.4570543	0.000132	3468.2	<.0001*
NeF_s1	0.3560012	0.000132	2701.4	<.0001*
GG_s1	0.2992776	0.000132	2271.0	<.0001*
GC_s1	-0.058089	0.000132	-440.8	<.0001*
FC_s1	-0.038543	0.000132	-292.5	<.0001*
(NeF_s1-1)*(NeF_s1-1)	0.1403629	0.002141	65.56	<.0001*
(GG_s1-1)*(GG_s1-1)	0.1216154	0.002141	56.81	<.0001*
(FHR_s1-1)*(FHR_s1-1)	-0.088568	0.002141	-41.37	<.0001*
(FHR_s1-1)*(NeF_s1-1)	0.0561434	0.002796	20.08	<.0001*
(GC_s1-1)*(GC_s1-1)	0.0408164	0.002141	19.07	<.0001*
(FC_s1-1)*(FC_s1-1)	0.0326969	0.002141	15.27	<.0001*
(FHR_s1-1)*(GC_s1-1)	-0.035812	0.002796	-12.81	<.0001*
(FHR_s1-1)*(FC_s1-1)	-0.034425	0.002796	-12.31	<.0001*
(FHR_s1-1)*(GG_s1-1)	0.0335012	0.002796	11.98	<.0001*
(GG_s1-1)*(NeF_s1-1)	-0.032808	0.002796	-11.74	<.0001*
(GC_s1-1)*(FC_s1-1)	0.0134005	0.002796	4.79	<.0001*
(NeF_s1-1)*(FC_s1-1)	0.0043899	0.002796	1.57	0.1268
(GG_s1-1)*(GC_s1-1)	0.0043898	0.002796	1.57	0.1268
(GG_s1-1)*(FC_s1-1)	0.0020794	0.002796	0.74	0.4628
(NeF_s1-1)*(GC_s1-1)	-0.002079	0.002796	-0.74	0.4628

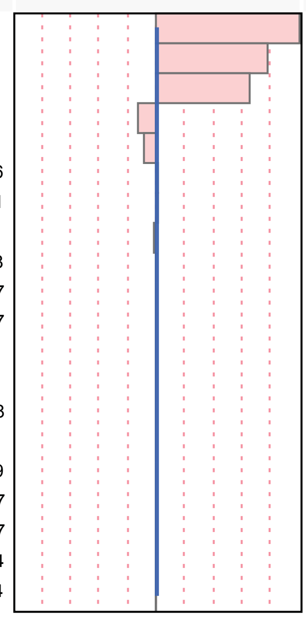

Fig. 4. Sorted parameter estimates (Eq. 3) for average fuel temperature.

III.B.2. Input sensitivity variation

As the thermal condition in AGR capsules is changing over the course of extended irradiation, the parameter sensitivities are also expected to change due to the nonlinearity of the thermal model equations. Therefore, the capsule thermal domain is divided into multiple smaller ranges, within which the output temperature can be estimated as a linear combination of input variables to satisfy Eq. 2 assumption. Data from AGR-2 Capsule 5 are used to show the variation of input sensitivity coefficients when the capsule thermal condition changes. Table I presents four scenarios (four different EFPDs) selected throughout the AGR-2 irradiation to cover the wide range of thermal conditions. The parameter sensitivity coefficients for VA FT and Peak FT are calculated as described in previous section for each scenario (see Table II). Fig. 5 shows that these sensitivity coefficients vary as functions of corresponding input variable. The daily sensitivity coefficients for the entire AGR-2 irradiation are estimated by substituting actual input variables to these functions.

Table I. Thermal conditions for four selected scenarios.

EPFD	Control gap size (mm)	Fuel heat rate (w/cm^3)	Fast fluence (n/m^{2}10^{25})	Neon fraction	Average fuel (°C)	Peak fuel (°C)
40	0.4003	65.01	0.23391	0.690	1,082	1,207
180	0.4219	93.32	1.02364	0.477	1,153	1,281
329	0.4463	117.50	1.91886	0.274	1,207	1,350
545	0.4785	67.46	3.10006	0.936	1,212	1,304

Table II. Parameter sensitivity for averaged and peak fuel temperatures**.**

Scenario	Response Variable	EFPD	Fuel Heat Rate (a_1)	Gas Gap (a_2)	Neon Fraction (a_3)	Graphite Conductivity (a_4)	Fuel Conductivity (a_5)
1	VA FT	40	0.457	0.299	0.356	-0.058	-0.039
	Peak FT	40	0.483	0.248	0.311	-0.080	-0.083
2	VA FT	180	0.533	0.272	0.206	-0.069	-0.053
	Peak FT	180	0.542	0.237	0.181	-0.086	-0.095
3	VA FT	329	0.556	0.252	0.102	-0.075	-0.064
	Peak FT	329	0.545	0.218	0.087	-0.088	-0.104
4	VA FT	545	0.469	0.200	0.433	-0.051	-0.036
	Peak FT	545	0.462	0.185	0.387	-0.062	-0.063

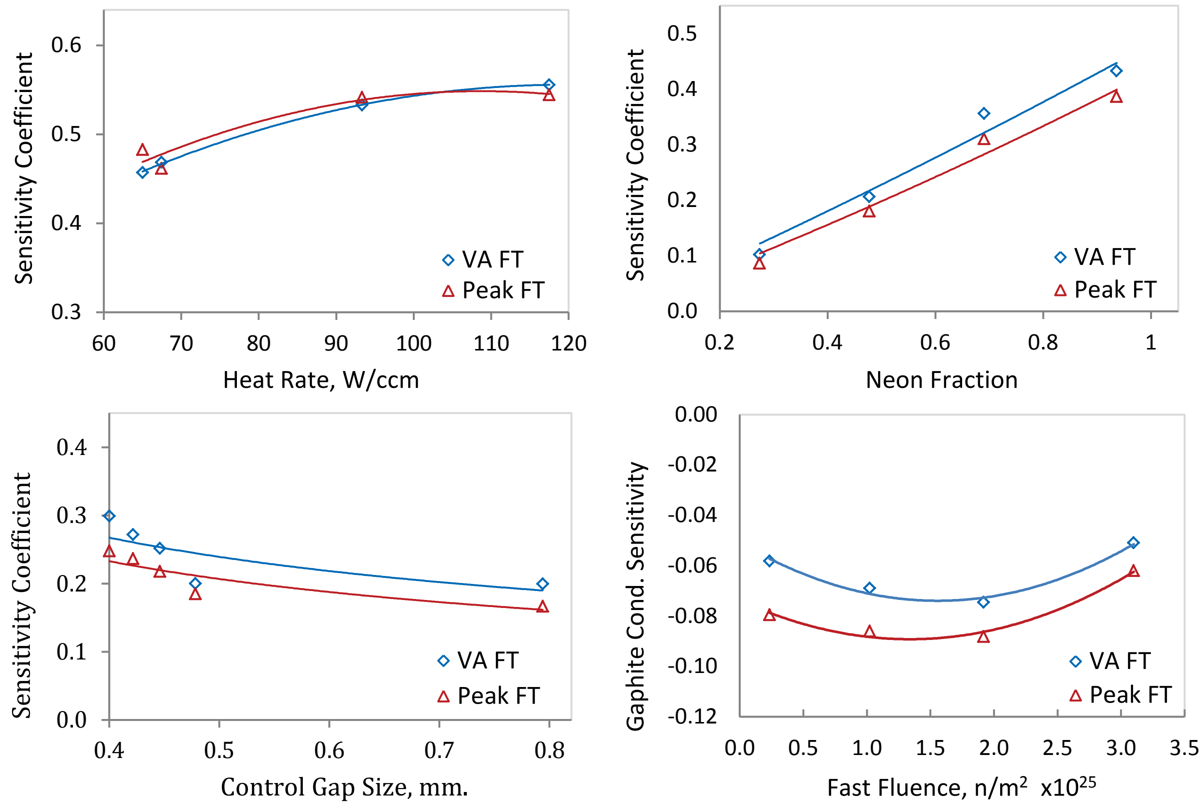

Fig. 5. Sensitivities for peak and average (VA) fuel temperatures as function of input.

III.C. Input Parameter Uncertainty

The daily uncertainties for fuel heat rate, fuel compact thermal conductivity, and graphite thermal conductivity were estimated by ART R&D program experts and modelers. They are assumed to be constant over the entire irradiation. However, the uncertainties of the control gap size and neon fraction are dynamic, accounting for the effect of unplanned events (e.g., gas line cross-talk failure occurred around middle of AGR-2 irradiation) and irradiation-induced changes in capsule thermal properties (e.g., gap variation due to graphite shrinkage). Fig. 6 shows an example of daily parameter uncertainties for AGR-2 Capsule 5, which are detailed in following subsections.

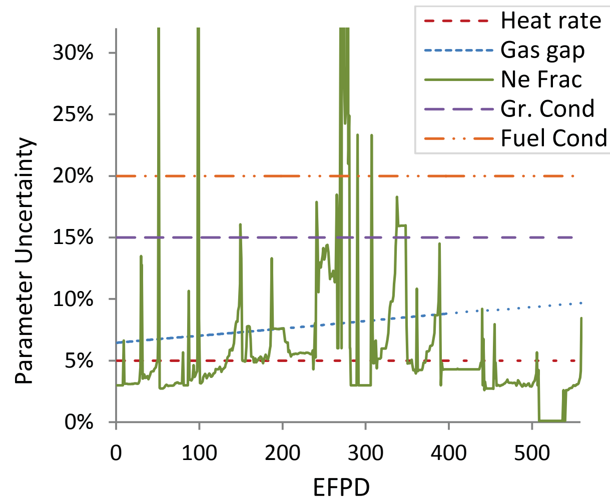

Fig. 6. AGR-2 Capsule 5 parameter uncertainties in terms of relative standard deviation.

III.C.1. Control gap size

At the beginning of irradiation the as-fabricated graphite holder outer diameter and capsule retainer sleeve inner diameter are adjusted, taking into account the thermal expansions when capsules are brought up to temperature. The "hot" control gap size, equal to a half of the difference between the above two adjusted diameters, is used in the ABAQUS model to predict temperatures in each capsule. At this point in time, the initial uncertainty of control gap size was based on machining tolerance and assumed to be about 0.0254 mm (or one-thousandth of an inch) for all capsules.

As the irradiation progresses, the post-irradiation examination metrology data of AGR-1 capsule components indicated that the graphite holders swelled unevenly (because of high boron addition to the graphite) for the four middle capsules (2–5), where the weight percent boron present in the material was 7% B4C. But, they shrank for Capsules 1 and 6 with lower boron concentrations of 5.5% B4C [12]. As a result, the control gap shrank for the four middle capsules and expanded for the top and the bottom capsules. This behavior is taken into account when calculating temperatures for all AGR capsules, such that the control gap is evenly and linearly changing over the entire irradiation beginning from initial hot gap size. The positive or negative rate of change depends on the boron concentration in the graphite holder. Thus, the control gap size for day i (Δx_i) can be calculated as a function of fast fluence [2]:

$$\Delta x_i = \Delta x_s + \alpha * r * ff_i \quad (5)$$

where Δx_s is start gap size, α is the rate of change (α=0.0018 for AGR-2 capsules [2]), *r* is the radius of graphite holder measured at fabrication, and ff_i is cumulative fluence in (10^{25} n/m^2) on day (*i*). Thus, the daily gap uncertainty (blue line in Fig. 6) is also assumed linearly increasing with cumulative fluence as:

$$\sigma_{G_i} = \sigma_{G_s} + \frac{ff_i}{ff_e}\left(\sigma_{G_e} - \sigma_{G_s}\right) \quad (6)$$

where σ_{G_i} is the gap size uncertainty on day (*i*); σ_{G_s} and σ_{G_e} are the gap size uncertainty at the start and end of irradiation assuming that $\sigma_{G_e} = 1.5 * \sigma_{G_s}$; and ff_e is cumulative fast fluence at the end of irradiation.

III.C.2. Neon fraction

For normal gas flow condition, the neon fraction is calculated as the ratio between neon flow rate (Q_{Ne}) and the sum of neon and helium flow rate (Q_{He}) as follows:

$$Nef = \frac{Q_{Ne}}{Q_{Ne}+Q_{He}} \quad (7)$$

Given the flow measurement uncertainty of 1 cm^3/min based on engineering assessment, a neon fraction simulation of Eq. 7, with neon and helium flows taken randomly from a normal distribution with the mean value and a standard deviation of 1 cm^3/min, was performed for different neon fraction levels. The neon fraction uncertainty for each neon fraction level is equal to the standard deviation calculated from 100,000 random neon fraction results. Then, the power equation of neon fraction is used to fit the calculated neon fraction uncertainties. As a result, the daily neon fraction uncertainty (green line in Fig. 6) is calculated by substituting the actual neon fraction in the following function:

$$\sigma_{Nef} = \frac{2.5487}{Nef^{1.047}} \quad (8)$$

More than halfway through AGR-2 irradiation, the gas line cross-talk failure occurred allowing the gas mixture from one capsule to enter other capsules; therefore Eq. 7 cannot be used to calculate neon fraction for each capsule. Instead, the neon fractions were estimated as a regression function of temperature defining parameters such as TC readings, fuel fission power, and fast fluence. However, the uncertainty of these predicted neon fractions can be relatively low because of the good fit between actual and predicted neon fractions, when capsule neon fractions can be accurately calculated during earlier cycles. As a conservative estimate, neon fraction uncertainty during cross-talk period is assumed to be double the normal neon fraction uncertainty. Fortunately, this cross-talk failure impacts neon fraction calculation for AGR-2 capsules only during period between 240 and 280 EFPDs as seen in Fig. 6.

III.C.3. Heat rate

The fuel heat rates are taken from the as-run physics calculation [7]. According to the modeler, the uncertainty in the calculated fuel heat rate is a collection of several factors from ATR measured data input parameters that go into the physics calculation and Monte Carlo statistical uncertainties associated with calculated parameters. These specific uncertainties include: (1) ATR total core or lobe power of ±4.1%; (2) fuel compact uranium beginning-of-life densities of ±0.5%; (3) calculated irradiation flux of ±1.0%; (4) calculated reaction rates or 1-group cross section of ±2.0%; (5) power normalization factors of ±1.0%; (6) outer shim control cylinder hafnium and beryllium reflector poison densities of ±1.0% ; and (7) outer shim control cylinder rotational position of ±0.5%. Assuming these individual uncertainties to be random, the daily overall fuel heat rate uncertainty can be estimated to be ±5.0% for all AGR capsules (red line in Fig. 6). In addition, good agreement between burnup calculated by the physics depletion model and post-irradiation examination measurements for AGR-1 experiment, where the difference is less than 10% for the worst compact, indicates that the fuel fission power uncertainty could be small.

III.C.4. Fuel compact and Graphite thermal conductivity

The fuel compact thermal conductivity was taken from correlations of conductivity with temperature, temperature of heat treatment, neutron fluence, and TRISO-coated particle packing fraction [13]. These correlations were further adjusted to account for differences in fuel compact density and packing fraction. The given correlations were developed for a fuel compact matrix density of 1.75 g/cm^3, whereas the compact matrix used in AGR had a lower density (i.e., approximately 1.6 g/cm^3 for UCO compacts and 1.68 g/cm^3 for UO_2 compacts in AGR-2 capsules). Thus, the thermal conductivities for AGR compacts were scaled according to the ratio of densities in order to correct for this difference. The lack of experimental data for AGR fuel compacts thermal properties leads to high uncertainty of compact thermal conductivity, which is estimated to be 20% (orange line in Fig. 6) for all AGR experiments.

Similarly, the unirradiated graphite thermal conductivity data for the holders were provided by GrafTech as a function of temperature and the weight percent boron carbide present in the material [13]. The effect of irradiation on the thermal conductivity of the graphite was accounted for in this analysis using the correlations which are obtained based on different graphite properties than the graphite employed in the AGR test trains. The fact that the thermal conductivity for the actual AGR graphite holder has to be extrapolated from given correlations also leads to high parameter uncertainty. However, according to expert assessment, the existence of one data point for validation of the correlation helps to reduce the graphite thermal conductivity uncertainty from an original estimated value of 20% to 15% (purple line in Fig. 6) for all AGR irradiations.

III.D. Correlation between Fuel Compact and Graphite Thermal Conductivities

For most of the input pairs, the noise correlation in Eq.2 can be assumed negligible because their noises are considered independent. However, the fuel and graphite thermal conductivities are both calculated as a function of temperature and fast fluence; therefore their noise correlation used in Eq. 2 is expected to be significant due to the same sources of variation. To estimate this noise correlation for each thermal condition (represented by [temperature, fluence] pairs), a hundred thousand fuel and graphite conductivities are calculated from the hundred thousand [temperature, fluence] pairs randomly sampled from their assumed normal noise distributions. The correlation coefficient between calculated graphite and fuel compact thermal conductivities is estimated using the JMP® “multivariate” function. The plot on the left of Fig. 7 shows scatter plot matrix of fuel temperature (Temp), fluence (*dpa)*, fuel (F Cond) and graphite thermal conductivities (G Cond) together with their noise distribution and pairwise correlation coefficients (r) calculated for the nominal temperature of 1200°C and fluence of 2.0 *dpa*. In this case correlation between fuel and graphite thermal conductivities is 0.96. Because the fuel and graphite temperature are maintained at the same level, the above procedure is repeated for different fluence levels covering entire range of each AGR irradiation as shown in the plot on the right of Fig. 7. The correlation between fuel and graphite conductivities as function of fast fluence can be expressed as follows:

$$\rho_{FC,GC} = -0.071ff^2 + 0.359ff + 0.446 \tag{9}$$

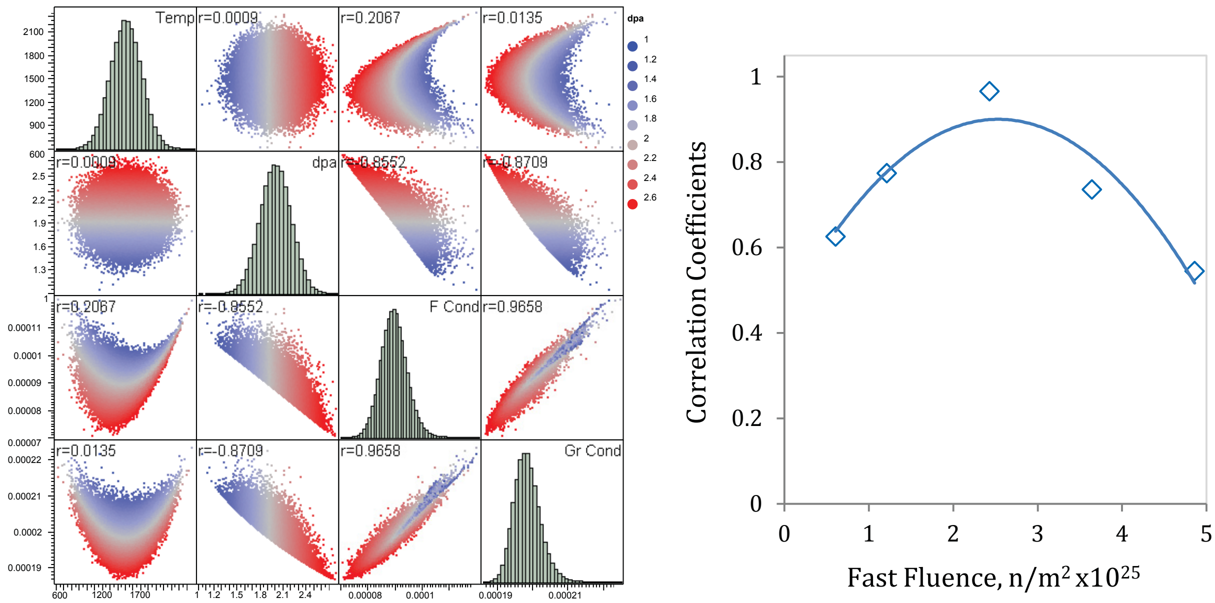

Fig. 7. Scatter plot matrix shows the correlation between fuel and graphite thermal conductivities (left) and correlations as function of fluence (right).

IV. UNCERTAINTY RESULTS

IV.A. Dominant Factors

The overall uncertainty of a calculated temperature in terms of variance is obtained through propagation of model parameter uncertainty as the summation of the parameter variances weighted by the squares of their sensitivity coefficients (Eq. 2). Thus, the effect of a parameter on the model prediction variation is a square of product of input uncertainty and the sensitivity coefficient. Fig. 8 shows the daily variances of peak FT and VA FT caused by the five significant input uncertainties for two representative capsules in AGR-2 test; Capsule 5 with smallest control gap (left plots) and Capsule 2 with hottest fuel temperature (right plots). The following conclusions are drawn:

- Fuel heat rate uncertainty of 5% is the most significant factor contributing to overall uncertainty of calculated peak and VA fuel temperatures (red lines) for both capsules.

- Fuel compact thermal conductivity uncertainty of 20% is a clear second most dominant factor for peak FT uncertainty in capsules with larger control gap (top right plot in Fig. 8 for Capsule 2), but has much less impact on VA FT uncertainty (orange lines).

- Graphite thermal conductivity uncertainty of 15% has relatively small impact on both peak and VA FT uncertainties (purple lines).

- Generally, neon fraction uncertainty has relatively small impact on fuel temperature uncertainty (green lines), except doubled neon fraction uncertainty caused by gas line cross-talk around 240 – 280 EFPDs makes it the second most influential factor in VA FT uncertainty during that time period (bottom row in Fig. 8).

- Higher relative uncertainty of control gap due to small gap size in Capsule 5 makes it the second most dominant factor for VA FT during most of irradiation except the cross-talk failure period (blue line on the bottom left plot in Fig. 8). The larger gap size in Capsule 2 reduces the relative gap uncertainty leading to insignificant impact of gas gap on calculated fuel temperature uncertainty.

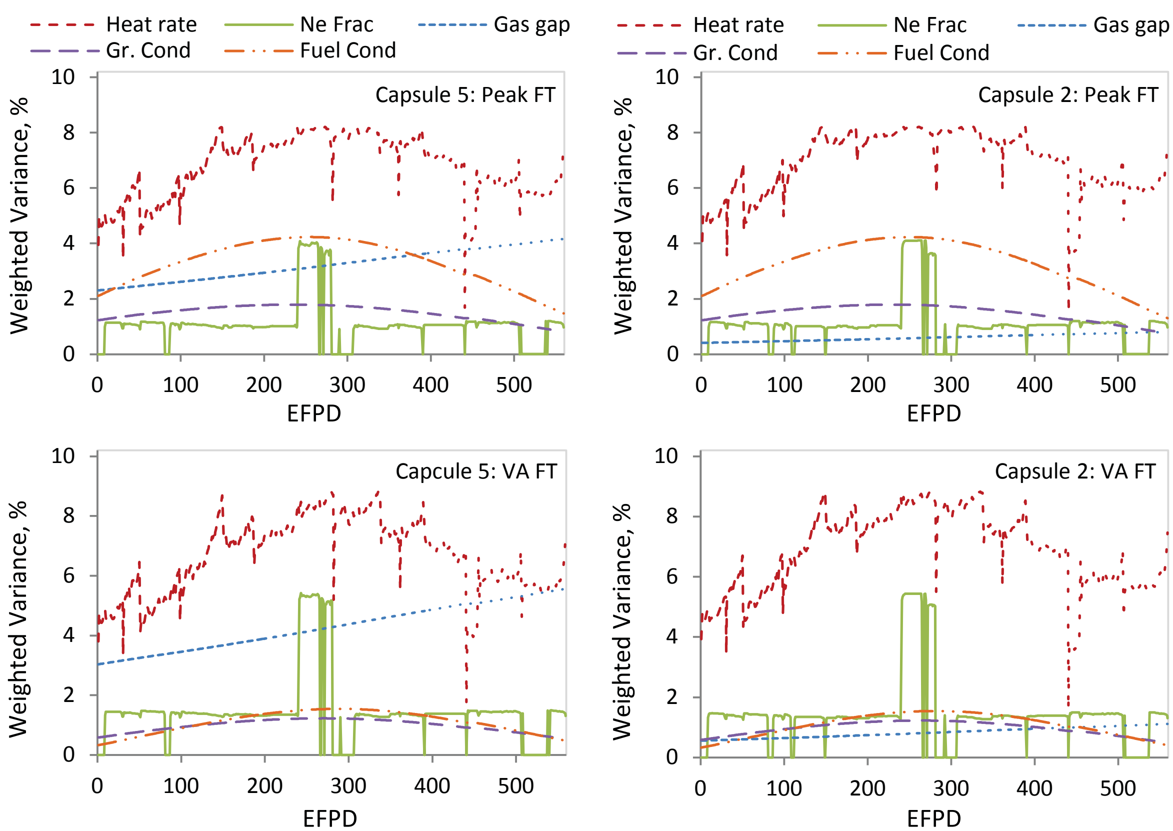

Fig. 8. Daily weighted temperature variances due to parameter uncertainties.

IV.B. Overall Calculated Temperature Uncertainty

The daily overall uncertainties in term of standard deviation for VA and peak fuel temperatures in Capsule 5, as a function of EFPD, are presented on the left of Fig. 9 and daily calculated temperatures with associated error bars of one standard deviation are plotted on the right of Fig. 9. These plots are similar for other capsules. Result highlights are:

- The peak FT uncertainty is higher than VA FT uncertainty largely due to higher impact of fuel thermal conductivity on peak FT as seen in Fig. 8. For AGR-2 capsules, the relative uncertainty ranged from 2.2% to 4.2% for VA FT (up to ~52°C) and ranged from 2.7% to 4.2% for peak FT (up to ~60°C).

- The overall uncertainty reaches highest values around midst of irradiation due to highest sensitivities of fuel heat rate (a dominant factor) and fuel and graphite thermal conductivities, when fuel heat rate reaches the peak level.

- The increase in neon fraction uncertainty due to gas line cross-talk failure around 240 – 280 EFPDs leads to an increase of about 5°C in fuel temperature uncertainty during that time.

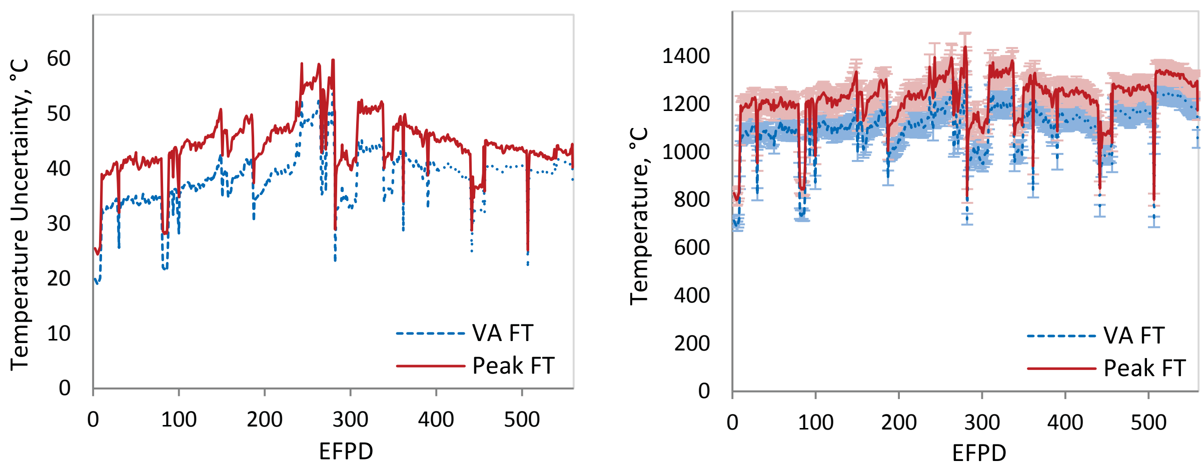

Fig. 9. AGR-2 Capsule 5 VA and peak fuel temperature daily uncertainties: Left – uncertainty in terms of standard deviation; Right - temperatures and uncertainty bars.

V. CONCLUSIONS

Knowledge of the thermal conditions and associated uncertainties of the nuclear fuel in a reactor test are central to the interpretation of the test results, and is necessary when using the test results for calibration and validation of nuclear fuel performance models and codes, ultimately in support of the design and licensing of the new nuclear fuel. This work focuses on quantification of calculated fuel temperature in AGR capsules due to input uncertainties. The thermal model parameters of potential importance to the predicted fuel temperatures are selected based on the combination of input uncertainty and sensitivity. Expert judgments are used as a basis to specify the uncertainty range for a set of select parameters taking into account all events that occurred during AGR-2 irradiation, which can impact input uncertainties (e.g., the cross-talk failure).

The parameter sensitivity defines how the predicted temperature would be influenced by changes in an input parameter. The sensitivity analysis performed in this work went beyond the traditional local sensitivity. Using experimental design, analysis of pairwise interactions of model parameters was performed to establish sufficiency of the first-order (linear) expansion terms in constructing the response surface. To achieve completeness, uncertainty propagation made use of pairwise noise correlations of model parameters. Further, using an interpolation scheme over the input parameter domain, the analysis obtains time-dependent sensitivity over the test campaign's duration. Propagation of model parameter uncertainty is then used to quantify the daily overall uncertainty of calculated fuel temperatures for the entire AGR irradiation. For example, for the AGR-2 capsules the relative uncertainty ranged from 2.2% to 4.2% for VA FT (up to ~52°C) and ranged from 2.7% to 4.2% for peak FT (up to ~60°C).

In addition to model-parameter uncertainties analyzed in this study, other epistemic uncertainties exist. In this case, these uncertainties can be categorized into three groups. The first group belongs to biases and errors in expert assessment of the range of uncertainty associated with input parameters. The second group includes modeling assumptions used to build the ABAQUS model for the AGR-2 test. The third group is associated with numerical treatment (e.g., discretization errors) needed to implement and operate the ABAQUS simulations. Although the effect of the first and second groups is generally very hard to evaluate, it is important to systematically delineate them, so not to over-state the confidence in predicted values (underestimating their uncertainties) stemming from a model-parameter uncertainty analysis alone.

ACKNOWLEDGMENTS

The authors would like to thank James Sterbentz and Nancy Lybeck of the Idaho National Laboratory (INL) for their supports and comments. This work is supported by the Very High Temperature Reactor Technology Development Office AGR Fuel Development and Qualification Program at INL under the U.S. Department of Energy contract DE-AC07-05ID14517.

REFERENCES

1. Idaho National Laboratory, *Technical Program Plan for the Very High Temperature Reactor Technology Development Office/Advanced Gas Reactor Fuel Development and Qualification Program*, PLN-3636 Rev 3, Idaho Falls, Idaho (2014).

2. G. Hawkes, J. Sterbentz, and B. Pham, “Thermal Predictions of The AGR-2 Experiment with Variable Gas Gaps,” *Proceedings of 2014 International Topical Meeting on Advances in Thermal Hydraulics (ATH’14)*, Reno, Nevada, June 15–19, 2014, Paper # 10218 (2014).

3. B.T. Pham, J.J. Einerson, and G.L. Hawkes, *Uncertainty Quantification of Calculated Temperatures for the AGR-1 Experiment*, INL/EXT-12-25169, Idaho National Laboratory (2013).

4. B.T. Pham, G.L. Hawkes, and J.J. Einerson, “Improving Thermal Model Prediction through Statistical Analysis of Irradiation and Post-Irradiation Data from AGR Experiments,” *Nuclear Engineering and Design* **271**, pp. 209-216 (2014).

5. G.L. Hawkes, J.W. Sterbentz, and B.T. Pham, “Sensitivity Evaluation of the Daily Thermal Predictions of the AGR-2 Experiment in the Advanced Test Reactor,” *Proc. of the ASME 2015 Power and Energy Conversion Conf.*, San Diego, California, June 28-July 2, 2015, paper# 49698 (2015).

6. G.L. Hawkes e. al., “Sensitivity Evaluation of the Daily Thermal Predictions of the AGR-1 Experiment in the Advanced Test Reactor,” *ICAPP 2011 Conference*, Nice, France (2011).

7. J. W. Sterbentz, et. al., “Monte Carlo Depletion Calculation for the AGR-1 TRISO Particle Irradiation Test,” *ANS Annual Conference*, San Diego, CA, June 2010, paper # 1308 (2010).

8. B.T. Pham and J.J. Einerson, “The statistical analysis techniques to support the NGNP fuel performance experiments,” *Nuclear Materials* **441 (**1–3), pp. 563–573 (2013).

9. B. Ostle and R. Mensing, *Statistics in Research*, 3rd Edition, Ames, Iowa: ISU Press (1975).

10. SAS, *JMP® 8 Statistics and Graphics Guide, Second Edition*. Cary, NC: SAS Institute Inc. (2009).

11. N. Draper and H. Smith, *Applied Regression Analysis*, John Wiley & Sons Inc., New York, USA (1966).

12. P. Demkowicz, e. al., “*AGR-1 Irradiated Test Train Preliminary Inspection and Disassembly First Look*,” INL/EXT-10-20722, Idaho National Laboratory (2011).

13. L. Snead and T. Burchell, “Reduction in Thermal Conductivity Due to Neutron Irradiation,” *22nd Biennial Conference on Carbon*, pp. 774-775 (1995).